

PAPER DETAILS

TITLE: The Effect of Production Parameters on Secondary Dendrite Arm Spacing (SDAS) and Estimation of Cooling Rate by SDAS in Functionally Graded Al-Cu Eutectic Alloy

AUTHORS: Semih Agca

PAGES: 36-41

ORIGINAL PDF URL: <https://dergipark.org.tr/tr/download/article-file/375017>

The Effect of Production Parameters on Secondary Dendrite Arm Spacing (SDAS) and Estimation of Cooling Rate by SDAS in Functionally Graded Al-Cu Eutectic Alloy[†]

Semih Ağca

*Department of Metallurgical and Materials Engineering, Ankara Yıldırım Beyazıt University, Turkey
agcasemih@gmail.com*

Abstract – In this study, the effect of production parameters (G number, casting atmosphere, and cooling rate) on secondary dendrite arm spacing (SDAS) and estimation of cooling rate by SDAS in functionally graded Al-Cu eutectic alloy are investigated. Functionally graded Al-Cu eutectic alloy is fabricated by centrifugal casting method. Different productions are carried out by changing cooling rate, G number and casting atmosphere. Cooling rate is controlled by a novel mold design and 0,09 K/s, 1,04 K/s, 1,96 K/s and 2,82 K/s cooling rates are obtained by using this mold. 10, 20 and 30 G numbers are obtained by changing the mold rotation speed. Air and 200 mBar vacuum atmospheres are preferred as casting atmospheres. SDASs are measured by Leica Application Suite V 4.6 image analysis software. Apparent interlamellar spacing is used in measurements. It is found that cooling rate alteration has a significant influence on SDAS. In addition to this, G number and casting atmosphere affected the SDAS by affecting the cooling rate. SDAS increased with the decreasing of cooling rate. Successful results are obtained in cooling rate estimation.

Keywords – Aluminum alloys, FGM, SDAS, cooling rate.

I. INTRODUCTION

Functionally graded aluminum alloys attracted the attention of scientists due to outstanding properties. There are many fabrication techniques for production of functionally graded materials. Powder metallurgy, thermal spraying and centrifugal casting are commonly used techniques for this process. Centrifugal casting differs from other techniques by being simple and cost effective. Rahvard et al. [1] have investigated the fabrication of A390 aluminum alloy by centrifugal casting with different magnesium contents and the characterization of the graded structures of samples. They found different particle distributions in the inner and outer layers and this affected the mechanical properties of samples. Lin et al. [2] have studied the fabrication of functionally graded Al-Si-Mg alloy by centrifugal casting. They showed that the functionally graded Al-Si-Mg alloy has superiority on conventional Al-Si-Mg alloy in wear resistance and thermal expansion property. Shailesh et al. [3] have studied the optimization of process parameters of Al-Si alloy by centrifugal casting. They found that the increase in the pouring temperature reduced mechanical properties; on the other hand, increase in mold speed increased the mechanical properties and density. Chirita et al. [4] have investigated the sensitivity of different aluminum alloys to centrifugal casting. They found that the centrifugal effect on mechanical properties was more pronounced in alloys with high eutectic contents. Mechanical properties of materials like hardness, tensile strength, percentage elongation, and impact energy are related with secondary dendrite arm spacing (SDAS) and SDAS can be controlled by cooling rate [5].

In this study, functionally graded Al-Cu eutectic alloy is fabricated by centrifugal casting. The effect of G number, casting atmosphere, and cooling rate on SDAS is investigated. Moreover, cooling rates of samples are roughly estimated by SDAS.

II. MATERIALS AND METHOD

A. Production of Pre-samples

Pure aluminium with ETIAL-7 standard and commercially pure copper are used to produce the Al-Cu eutectic alloy. Chemical composition of ETIAL-7 aluminium is shown in Table 1.

Table 1. Chemical composition of ETIAL-7 aluminium

Element	Al	Fe	Si	Cu	Others
Weight (%)	99.7	0.15	0.25	0.03	0.17

Chemical composition of commercially pure copper is shown in Table 2.

Table 2. Chemical composition of commercially pure copper

Element	Cu	Fe	Si	Bi	S	Others
Amount	+99.99 Wt. %	<2.00 ppm	<2.00 ppm	<2.00 ppm	<10.00 ppm	<15.00 ppm

Aluminum and copper are weighted according to eutectic ratio and melted in SiC crucible at 700°C by an electrical resistance melting furnace. Liquid metal stirred with pure copper sticks to avoid contamination and for having a homogenous eutectic melt. Chemical compositions of pre-samples are tested by optical emission spectrometer to be sure about homogeneity. The result is shown in Table 3.

[†] This is an extended version of a conference paper (ISMSIT2017).

Table 3. Chemical composition of Al-Cu eutectic alloy pre-samples

Element	Al	Cu	Si	Fe	Others
Weight (%)	66.90	32.80	0.03	0.15	0.05

The centrifugal casting machine that used in this study has a closed system, so material adding is impossible while working. For this reason, pre-samples are produced in steel molds those have same volume with the centrifugal casting mold. Pre-samples and steel molds are shown in Fig. 1.



Fig. 1. Pre-samples and steel molds

B. Mold Design

Four different molds are designed by using metallic and ceramic materials. Outer parts of molds are fabricated from Al-6061 alloy to protect molds from the negative effects of high pressure that occurs in centrifugal casting process. Copper coolers are located on the bottom of molds. Different cooling rates are obtained by changing the contact area between liquid alloy and the copper cooler. Inner parts of molds are fabricated from ceramic materials with low heat transfer coefficients. Mold designs are shown in Fig. 2.

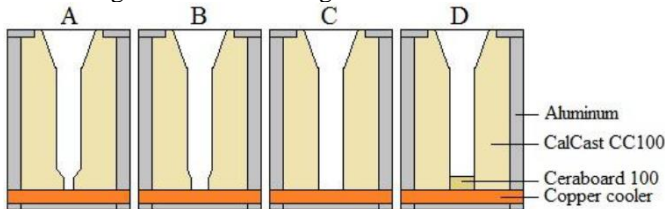


Fig. 2. Mold designs for obtaining different cooling rates

Calcast CC100 is used in inner parts of A, B, C, and D molds. Furthermore, Ceraboard 100 is used in D mold to prevent the contact of liquid alloy to copper cooler. Directional solidification is obtained in A, B, and C molds by the difference between heat transfer coefficients of Calcast CC100 and copper cooler. There was no directional solidification in D mold because of equal heat transfer in all directions. Heat transfer coefficients of mold materials are shown in Table 4.

Table4. Heat transfer coefficients of mold materials [6, 7]

Material	Cu	Al-6061	Calcast CC100	Ceraboard 100
Heat transfer coefficient(W/mK)	400	167	0.26	0.13

Cooling rates and the contact areas between liquid alloy and the copper coolers are shown in Table 5.

Table5. Cooling rates of molds and contact areas

Mold	A	B	C	D
Cooling Rate(K/s)	1.04	1.96	2.82	0.09

Contact Area(cm ²)	2.35	4.70	7.05	none
--------------------------------	------	------	------	------

Detailed information about molds and heat transfer calculations can be found in another study [8].

C. Centrifugal Casting

Functionally graded Al-Cu eutectic alloy samples are fabricated by casting pre-samples in TopCast TCE centrifugal casting machine. Centrifugal casting machine and mold are shown in Fig. 3.

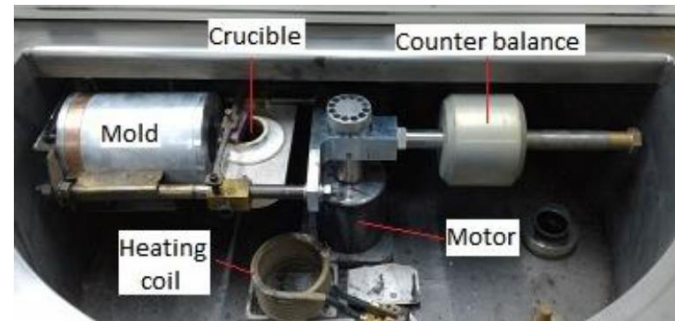


Fig. 3. Centrifugal casting machine and mold

Mold rotation speed is set to achieve 10, 20 and 30 G numbers. Ceramic parts of the mold are pre-heated to 200°C to avoid the thermal shock and cracking. 700°C is selected for casting temperature and controlled by optical pyrometer. After putting the pre-sample to crucible, the cover of centrifugal casting machine is closed and 200 mBar vacuum is applied to all specimens for degassing until completion of melting. Vacuum is released before rotation in fabrication of specimens produced in air atmosphere and held until the end of rotation for specimens fabricated in vacuum atmosphere. After the melt reached 700°C, mold is rotated for 8 and 15 minutes for high cooling rates (A, B, and C molds) and slow cooling rate (D mold), respectively. These time slots include pouring, solidification and cooling. Fabricated samples by A, B, C, and M molds are shown in Fig. 4.

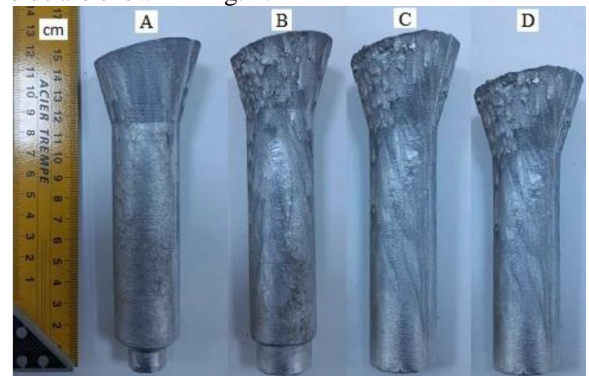


Fig. 4. Fabricated samples by A, B, C, and D molds

D. Metallographic Examination

Fabricated samples are cut into pieces by abrasive cutter like shown in Fig. 5 to make more feasible for metallographic examination.

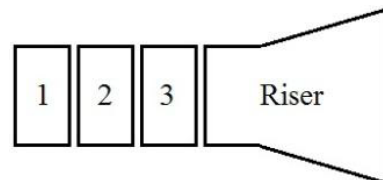


Fig. 5. Pieces of samples

All pieces are cut through the axis of symmetry to investigate the interior parts of samples. After cutting, samples are grinded with 320, 600, 800, 1000, and 1200 grit SiC abrasive papers.

Samples are polished and etched by Struers LectroPol-5 electropolisher for 5 seconds at 22°C. The volumetric ratios of components of electrolyte used in electropolishing are shown in Table 6.

Table6. Components of electrolyte used in electropolishing

Component	Vol %
Ethyl alcohol	60
Distilled water	20
2-Butoxyethanol	15
HClO ₄ (perchloric acid)	5

After electropolishing, microstructure photographs are taken by Leica DMI5000M microscope.

E. SDAS Measurement

SDAS measurements are practiced by Leica Application Suite V 4.6 image analysis software. Apparent interlamellar spacing is used in measurements. Fig. 6 shows apparent and random interlamellar spacings.

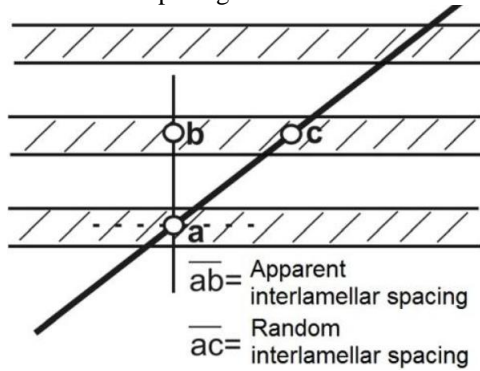


Fig. 6. Apparent and random interlamellar spacings [9]

F. Cooling Rate Estimation

Cooling rates of samples are roughly estimated by the equation shown below.

$$\text{Cooling rate} = \left(\frac{\Delta h_f}{C_p} \right) \times \left(\frac{2K}{R\lambda^2} \right)$$

Δh_f is latent heat, C_p is specific heat, K is the constant equals $27.5 \times 10^{-12} \text{ cm}^3/\text{s}$ obtained from unidirectional solidification experiments for the Al-Cu eutectic alloy. R is the radius of the cylinder sample (15 mm) and λ is SDAS interlamellar spacing. $\Delta h_f / C_p$ equals 440 K for the Al-Cu eutectic alloy [10].

III. RESULTS

Cooling rate alteration has a significant influence on SDAS. In addition to this, G number and casting atmosphere affected the SDAS by affecting the cooling rate.

Small SDASs occurred after the fabrication with high cooling rate. On the other hand, big SDASs developed after low cooling rate fabrications. Microstructures of samples fabricated in different cooling rates are shown in Fig. 7.

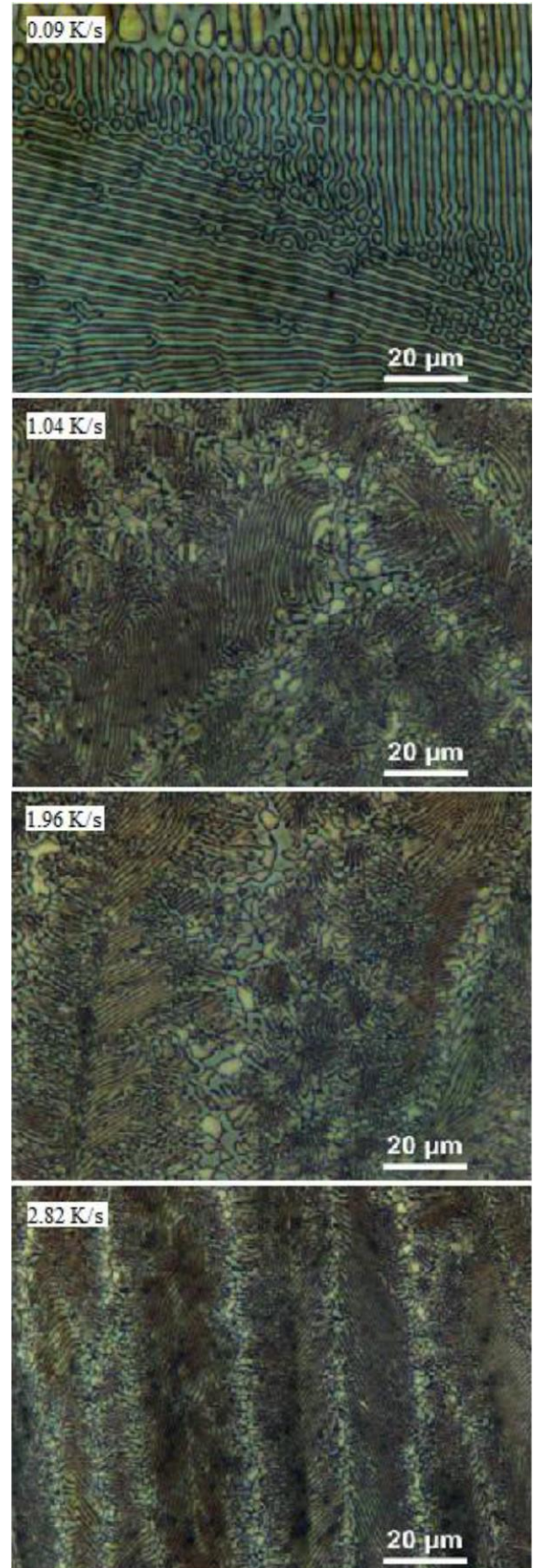


Fig. 7. Microstructures of samples fabricated in different cooling rates

The biggest SDASs are obtained with 0.09 K/s cooling rate, and the smallest SDASs are obtained with 2.82 K/s cooling rate.

Since A, B, and C molds are designed for directional solidification, both SDAS and solidification direction changed

in different parts of samples fabricated by these molds. Solidification directions and SDASs of different parts of samples fabricated by A, B, and C molds are shown in Fig. 8.

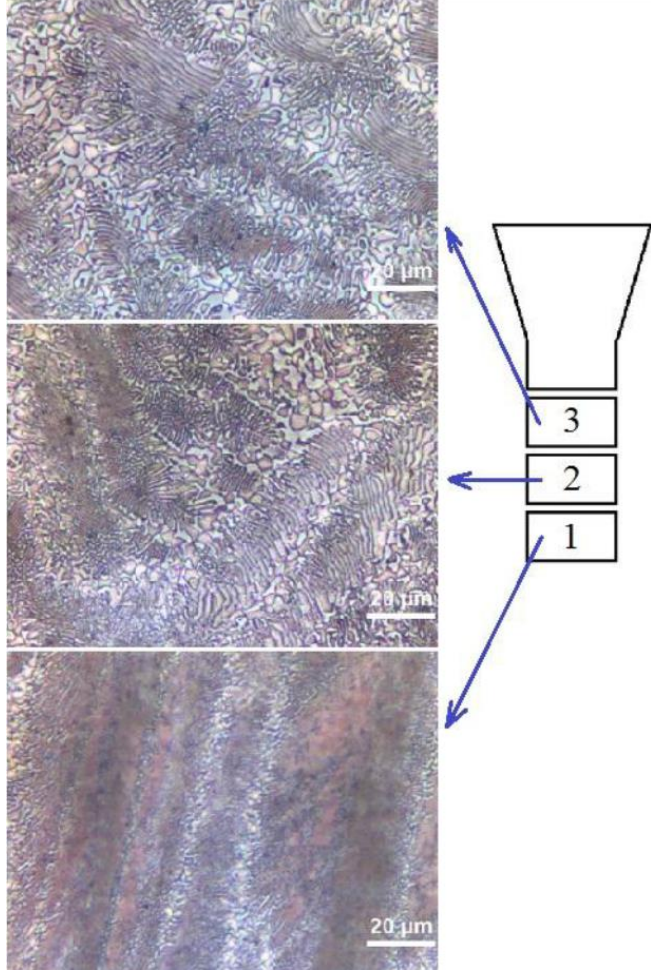


Fig. 8 Microstructures of different parts of samples (A, B, and C molds)

It is obvious that, first part has the smallest SDAS, and third part has the biggest. Moreover, the solidification direction is towards the copper cooler in first part, and it changes its direction as moving away from copper cooler. SDASs of samples fabricated by A mold are shown in Fig. 9.

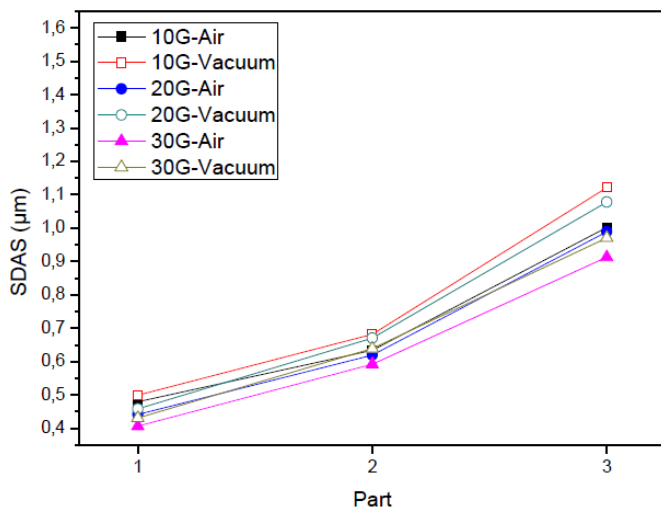


Fig. 9 SDASs of samples fabricated by A mold

As can be seen from Fig. 9, the SDAS values of third part are bigger than SDAS values of other parts. SDAS becomes

smaller with increasing of G number. SDAS values of samples fabricated in vacuum atmosphere are bigger than those of fabricated in air atmosphere. SDASs of samples fabricated by B mold are shown in Fig. 10.

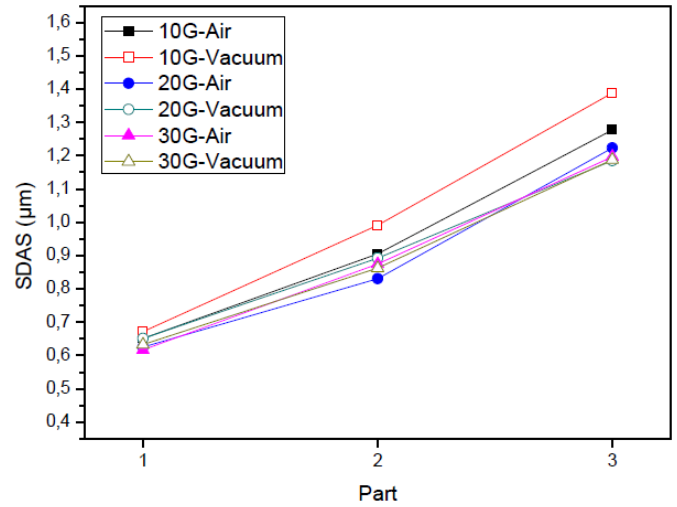


Fig. 10. SDASs of samples fabricated by B mold

As the cooling rate increases, SDAS decreases. SDASs of first parts of samples fabricated by A mold are in the range of 0.8-0.9 µm. This range decreased to 0.6-0.7 µm in the first parts of samples produced by B mold because of the increasing of cooling rate from 1.04 K/s to 1.96 K/s. This situation is also valid for second and third parts. SDASs of samples fabricated by C mold are shown in Fig. 11.

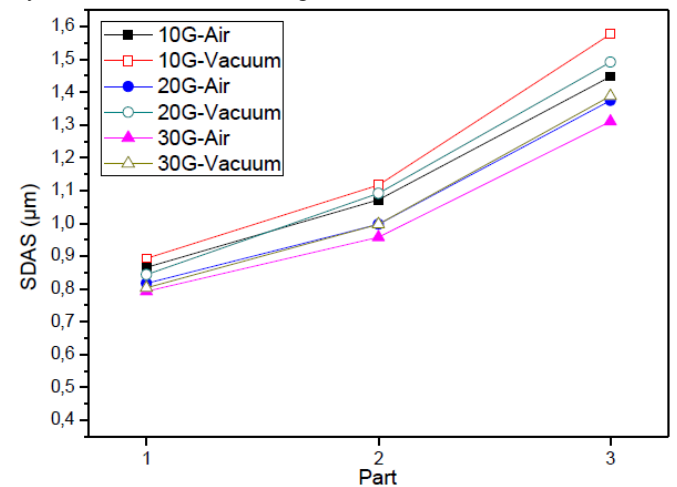


Fig. 11 SDASs of samples fabricated by C mold

As the cooling rate increased to 2.82 K/s, SDASs in the first parts of samples decreased to the range of 0.4-0.5 µm. It decreased to the range of 0.6-0.7 µm in second parts and 0.9-1.1 µm in third parts. The effects of G number and casting atmosphere on SDAS are similar in A, B, and C molds. In addition to this, the effects of G number and casting atmosphere decreased very little with the increasing of cooling rate.

In the A, B, and C molds, there is a difference between SDAS values of different parts. This situation is due to the decreasing temperature gradient from the copper cooler to the riser zone in the A, B, and C molds. SDASs of samples fabricated by D mold are shown in Fig. 12.

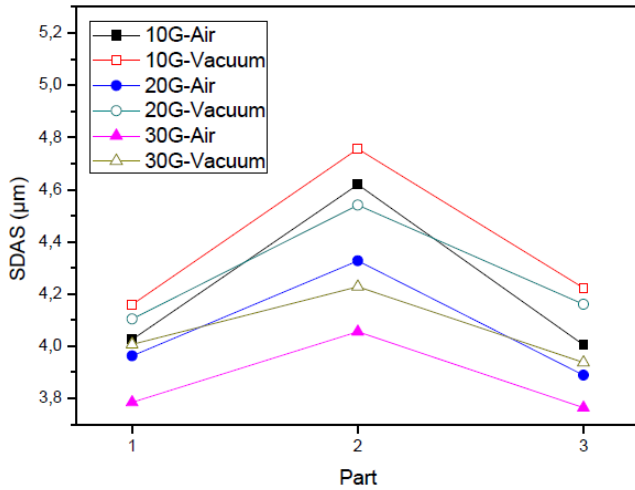


Fig. 12 SDASs of samples fabricated by D mold

As can be seen from Fig. 12, while SDASs in first and third parts are in the range of 3.7-4.3 μm , it is in the range of 4.0-4.8 in second parts. The effects of G number and casting atmosphere on SDAS are similar with the samples fabricated in high cooling rates. SDAS decreased with increase of G number and increased with vacuum application. In addition to this, G number and casting atmosphere are more effective in low cooling rate. Longer fluid retention of the alloy at low cooling rate is the main reason for the increase in G number and casting atmosphere effects.

To make an appropriate comparison between calculated and estimated cooling rates, mean value of SDASs from first, second, and third part is used in estimations. Mean values of SDASs of different parts are shown in Table 7.

Table7. Mean values of SDASs of different parts

Process\Mold	A	B	C	D
10G-A	1.128 μm	0.944 μm	0.705 μm	4.216 μm
10G-V	1.195 μm	1.017 μm	0.767 μm	4.379 μm
20G-A	1.063 μm	0.893 μm	0.683 μm	4.059 μm
20G-V	1.142 μm	0.909 μm	0.735 μm	4.268 μm
30G-A	1.020 μm	0.896 μm	0.637 μm	3.868 μm
30G-V	1.062 μm	0.894 μm	0.680 μm	4.057 μm

Mean values of SDASs are used as λ in cooling rate estimation equation. Estimated cooling rate results are shown in Table 8.

Table7. Mean values of SDASs of different parts

Process\Mold	A	B	C	D
10G-A	1.268 K/s	1.810 K/s	3.240 K/s	0.090 K/s
10G-V	1.129 K/s	1.560 K/s	2.740 K/s	0.084 K/s
20G-A	1.427 K/s	2.020 K/s	3.450 K/s	0.098 K/s
20G-V	1.237 K/s	1.950 K/s	2.980 K/s	0.088 K/s
30G-A	1.550 K/s	2.010 K/s	3.970 K/s	0.100 K/s
30G-V	1.430 K/s	2.018 K/s	3.480 K/s	0.098 K/s

As can be seen from Table 8 and Table 5, estimated and calculated cooling rates are similar with 11.5 % error in total.

IV. DISCUSSION

The difference in solidification direction between the parts is due to the different cooling rates of these parts. There is a decreasing temperature gradient in the A, B, and C molds from the copper cooler to the riser zone. Thus, the temperature difference which is the driving force of directional

solidification decreases and this changes the solidification direction.

Vacuum allows the alloy to remain liquid for a longer period of time because it reduces the number of air molecules in the environment and prevents heat transfer by convection. In the samples fabricated in vacuum atmosphere, the SDAS is bigger due to the longer completion of the solidification.

The effect of the G number can be defined by changing the cooling rate. As the G number increases, the pressure applied to the liquid metal increases. The increase in pressure applied to the liquid metal allows for better contact in the liquid metal-mold interface and faster transfer of heat from this interface. Thus, solidification becomes faster and SDAS becomes smaller [11].

Since the contact of liquid metal and copper cooler is prevented by isolation material, there is no decreasing temperature gradient from the copper cooler to the riser zone in D mold. However, a new temperature gradient occurred by different heat losses. First and third parts lost more heat than second part, so second part remained hot. This situation caused a new temperature gradient increasing from first part to second part, and decreasing from second part to third part. This temperature gradient changed the cooling rates of different parts and SDASs.

The error in cooling rate estimations derived from heat transfer calculations, measurement of SDASs only from three part, and image analysis software. The total errors in other cooling rate estimation studies in literature are between 15 % and 20 % [12]. Consequently, 11.5 % total error can be accepted as successful.

V. CONCLUSION

Functionally graded Al-Cu eutectic alloy is fabricated successfully with SDAS and solidification direction gradations.

The effect of production parameters on SDAS is revealed. Cooling rate is the most dominant parameter for SDAS change. G number and casting atmosphere are affected SDAS by affecting cooling rate in different ways.

The difference between SDASs of different parts of samples is derived from temperature gradation in molds. Different temperature gradations occurred due to different mold designs.

When compared with other studies from literature, successful cooling rate estimation results are obtained.

ACKNOWLEDGMENT

This work was supported by Nev Vakumlu Hassas Döküm (Newincasting). This technical support was gratefully acknowledged.

REFERENCES

- [1] S. M. [1] M. M. Rahvard, M. Tamizifar, S. M. A. Boutorabi, and S. G. Shiri, "Characterization of the graded distribution of primary particles and wear behavior in the A390 alloy ring with various Mg contents fabricated by centrifugal casting," *Materials and Design*, vol. 56, pp. 105-114, 2014.
- [2] X. Lin, C. Liu, and H. Xiao, "Fabrication of Al-Si-Mg functionally graded materials tube reinforced with in situ Si/Mg₂Si particles by centrifugal casting," *Composites: Part B*, vol. 45, pp. 8-21, 2013.
- [3] P. Shailesh, S. Sundarajan, and M. Komaraiah, "Optimization of process parameters of Al-Si alloy by centrifugal technique using

- Taguchi design of experiments,” *Procedia Materials Science*, vol. 6, pp. 812-820, 2014.
- [4] G. Chirita, I. Stefanescu, D.Cruz, D. Soares, and F. S. Silva, “Sensitivity of different Al-Si alloys to centrifugal casting effect,” *Materials and Design*, vol. 31, pp. 2867-2877, 2010.
- [5] M. Ş. Turhal and T. Savaşkan, “Relationships Between Secondary Dendrite Arm Spacing and Mechanical Properties of Zn-40Al-Cu Alloys,” *Journal of Materials Science*, vol. 38, pp. 2639-2646, 2003.
- [6] Y. Çengel, *Introduction to Thermodynamics and Heat Transfer* (2nd Ed.), USA: McGraw-Hill Primis, 2008.
- [7] J. A. Vargas, J. E. Torres, J. A. Pacheco, and R. J. Hernandez, “Analysis of heat input effect on the mechanical properties of Al-6061-T6 alloy weld joints,” *Materials and Design*, vol. 52, pp. 556-564, 2013.
- [8] S. Ağca and N. Akar, “Santrifüj Döküm Yöntemiyle Üretilen Al-Cu Fonksiyonel Derecelenmiş Malzemelerde Üretim Parametrelerinin Malzemenin Sertliği Üzerine Etkisi,” *Politeknik Dergisi*, vol. 20(1), pp. 121-127, 2017.
- [9] A. Czarski and P. Matusiewicz, “Some aspects of estimation accuracy of mean true interlamellar spacing,” *Metallurgy and Foundry Engineering*, vol. 38(2), pp. 133-140, 2012.
- [10] T. Koziel, P. Matusiewicz, M. Kopyscianski, and A. Zielinska-Lipiec, “Estimation of the cooling rate in 3 mm suction-cast rods based on the microstructural features,” *Metallurgy and Foundry Engineering*, vol. 39(2), pp. 7-14, 2013.
- [11] N. Akar, K. Boran, and B. Hoziklişil, “Effect of mold temperature on heat transfer coefficient at casting-mold interface,” *Journal of the Faculty of Engineering & Architecture of Gazi University*, vol. 28(2), pp. 275-282, 2013.
- [12] Y. Watanabe, Y. Hattori, and H. Sato, “Distribution of microstructure and cooling rate in Al-Al₂Cu functionally graded materials fabricated by a centrifugal method,” *Journal of Materials Proces*